Article ID: 1671-3664(2006)01-0093-09

3D viscous-spring artificial boundary in time domain

Liu Jingbo(刘晶波)[1†], Du Yixin(杜义欣)[1‡], Du Xiuli(杜修力)[2†], Wang Zhenyu(王振宇)[1§] and Wu Jun(伍俊)[1§]

1. *Department of Civil Engineering, Tsinghua University, Beijing 100084, China*
2. *Beijing Lab of Earthquake Engineering and Structural Retrofit, Beijing University of Technology, Beijing 100022, China*

Abstract: After a brief review of studies on artificial boundaries in dynamic soil-structure interaction, a three-dimensional viscous-spring artificial boundary (VSAB) in the time domain is developed in this paper. First, the 3D VSAB equations in the normal and tangential directions are derived based on the elastic wave motion theory. Secondly, a numerical simulation technique of wave motion equations along with the VSAB condition in the time domain is studied. Finally, numerical examples of some classical elastic wave motion problems are presented and the results are compared with the associated theoretical solutions, demonstrating that high precision and adequate stability can be achieved by using the proposed 3D VSAB. The proposed 3D VSAB can be conveniently incorporated in the general finite element program, which is commonly used to study dynamic soil-structure interaction problems.

Keywords: artificial boundary; viscous-spring; wave motion; time domain; numerical simulation; soil-structure interaction

1 Introduction

Numerical simulation methods for near-field wave motion problems have developed rapidly since the 1970s. Near-field wave motion problems, such as foundation vibration, dispersion of earthquake waves, blast engineering, etc., can all be considered as soil-structure interaction problems (Liao, 1997, 2002; Liu, 2002). Numerical techniques are widely used to solve transient wave motion problems in infinite or semi-infinite domains. If a verified virtual artificial boundary condition is introduced into the numerical method, the problem can then be solved in a finite computing domain instead of an infinite medium. The equations of motion and physical boundary conditions can be discretized by using the finite element method (FEM) or finite difference method (FDM). The simulation of wave motion thus becomes primarily an arithmetic problem, and simulation of the practical wave motions can be carried out by using the general FEM directly. Obviously, constructing an accurate artificial boundary condition (ABC) is necessary to enable this process. The essence of the artificial boundary is that the boundary is able to efficiently absorb the energy of the scattering waves, from the generalized structure to the infinite media. Based on this idea, extensive studies on artificial boundary problems have been carried over the past 30 years (Wolf, 1986; Liao, 1997; Kausel, 1988). There are two main directions in these studies, the global ABC and the local ABC. The global ABC has high accuracy, but its techniques can be quite costly and time consuming to implement due to the coupling characteristics of spatial and time domains. Therefore, for large-scale models, global ABCs may not be available. A seismic free field input formulation of the coupling procedure of the finite element and the scaled boundary finite element is proposed to perform the unbounded soil-structure interaction analysis in time domain (Yan *et al*., 2003). It uses a fast eigen system realization system, which significantly reduces the computational effort. On the other hand, local ABCs are important due to their decoupling characteristics of time and spatial domains.

In developing a local ABC, the earlier viscous boundary was widely applied due to its clearly presented concept and convenient implementation. A viscous boundary was first proposed by Lysmer and Kulemeyer (1969). It is equal to the viscous dampers applied on the boundary to absorb energy of the incident waves. Lysmer's viscous boundary was recommended in the *Chinese code for seismic design of nuclear power plants* (GB50267-97). However, the viscous boundary considers only the absorption of energy from scatter

Correspondence to: Liu Jingbo, Department of Civil Engineering, Tsinghua University, Beijing 100084, China. Tel: 86-10-62772988; Fax: 86-10-62771132
E-mail: Liujb@tsinghua.edu.cn
[†]Professor; [‡]Graduate Student; [§]Ph.D.

Supported by: National Natural Science Foundation of China Under Grant No.50478014; Special Funds for Major State Basic Research Project Under Grant No.2002CB412706; Research Funds from National Civil Defense Office of China for the Tenth Five-year Plan
Received December 3, 2005; **Accepted** February 26, 2006

waves. From physical concepts, a mechanical model with a viscous boundary is a separated body, which is suspended in space. The entire model can shift as a rigid body under low frequency force. A viscous boundary derived from a one-dimensional wave motion theory would result in large errors when it is applied to a multi-dimensional situation (Liu, 1997). Henceforth, scholars derived many types of local ABCs; only some are introduced in this paper. A nonreflecting plane boundary proposed by Smith (1974) was a superposition boundary based on the reflection characteristics of a plane wave on fixed and free boundaries. Liao derived a transmitting boundary based on the simulation of the propagation procedure of various one-way waves. This type of ABC can be applied to a linear combination problem of any one-way wave propagation problem without modification. Foreman (1986), Higdon (1986) and Keys(1985) derived a Clayton-Enquist absorbing ABC by using the sound wave equation. This type of ABC is a paraxial approximate transmission boundary. Zhao *et al*. (1989) proposed an infinite element boundary to deal with the infinite basement problem. Deeks and Randolph (1994) presented a type of 2D viscous-spring boundary.

The local ABC is applied in civil engineering to solve soil-structure interaction (SSI) problems. The ABC derived from wave motion theory could not simulate a zero-frequency component, e.g., the static component. Many scholars tried to use local ABC to solve static problems encountered in the study of SSI. Underwood and Green (1981) set up a doubly asymptotic boundary element method by combining static and viscous boundaries. This type of boundary can simulate zero-frequency and infinite-frequency problems accurately, but had only one-order of accuracy for the other frequencies problems. Wolf and Song (1995) proposed a type of doubly asymptotic unbounded media-structure interaction analysis method. Jing and Liao(2000) and Liao (2002) combined static boundary and multi-transmitting formula to solve the problem. This method can be used with various numerical methods directly in the near field. The aforementioned ABCs are not accurate enough to be used in engineering and are too complicated to be applied in numerical simulation. To overcome these shortcomings, Deeks and Randolph (1994) developed an axisymmetric transmitting boundary for the 2D case in the time domain based on the cylindrical wave theory. The 2D in-plane tangential boundary condition with viscous springs developed by Liu and Lu (1997, 1998) was perfected. Liu also discussed the merits of this boundary by comparing it with other boundaries, such as enabling the simulation of the elastic restoring performance of the semi-infinite media out of the artificial boundary. The viscous spring boundary is more stable in simulating the high or low frequency problem.

However, practical wave motion problems are always three-dimensional. If a low dimensional boundary is applied to a multi-dimensional situation, the results would be highly unrealistic. Therefore, to develop a 3D viscous spring boundary and its numerical simulation method is important.

Based on the theory of elastic waves in the near-field, 3D viscous spring artificial boundary (VSAB) equations are derived and their numerical simulation technique is presented in this paper. To verify the proposed 3D VSAB's reliability and practicality, numerical examples of some classical elastic wave motion problems are presented and the results are compared with the associated theoretical solutions. These comparisons demonstrate that a high degree of precision and adequate stability can be achieved.

2 3D VSAB condition in normal direction

2.1 Boundary equations in normal direction

Equation (1) is the wave motion equation of spherical expanding wave (P wave) in spherically symmetrical coordinates.

$$\frac{\partial^2(R\phi)}{\partial R^2}=\frac{1}{c_{\mathrm{p}}^2}\frac{\partial^2(R\phi)}{\partial t^2} \tag{1}$$

where ϕ is the potential function of displacement, c_{p} is P wave velocity of the media and R is the radial coordinate. The general solution of Eq.(1) is

$$\phi(R,t)=\frac{1}{R}f(R-c_{\mathrm{p}}t)+\frac{1}{R}g(R+c_{\mathrm{p}}t) \tag{2}$$

where, $f(\cdot)$ and $g(\cdot)$ are functions expressing scattering wave and converging wave, respectively.

The displacement normal to the wave front can be expressed as follows if the scattering wave is taken into consideration (Wolf, 1988).

$$u=\nabla\phi=\frac{\partial\phi}{\partial R}=\frac{1}{R}f'(R-c_{\mathrm{p}}t)-\frac{1}{R^2}f(R-c_{\mathrm{p}}t) \tag{3}$$

The normal stress is computed by the following equation.

$$\sigma=(\lambda+2\mu)\frac{\partial u}{\partial R}+2\lambda\frac{u}{R} \tag{4}$$

with λ and μ being Lamé constants. From Eq.(3),

$$\frac{\partial u}{\partial R}=\frac{1}{R}f''(R-c_{\mathrm{p}}t)-\frac{2}{R^2}f'(R-c_{\mathrm{p}}t)+\frac{2}{R^3}f(R-c_{\mathrm{p}}t) \tag{5}$$

$$\frac{u}{R}=\frac{1}{R^2}f'(R-c_{\mathrm{p}}t)-\frac{1}{R^3}f(R-c_{\mathrm{p}}t) \tag{6}$$

Substituting Eqs.(5) and (6) into Eq.(4), the normal stress on the wave front expressed by function $f(\cdot)$ is obtained.

$$\sigma = \frac{\lambda + 2\mu}{R} f^{''}(R - c_{\mathrm{p}}t) - \frac{4\mu}{R^2} f^{'}(R - c_{\mathrm{p}}t) + \frac{4\mu}{R^3} f(R - c_{\mathrm{p}}t) \tag{7}$$

Introducing the following functions into Eq. (7),

$$\dot{u} = \frac{\partial u}{\partial t} = -\frac{c_{\mathrm{p}}}{R} f^{''}(R - c_{\mathrm{p}}t) + \frac{c_{\mathrm{p}}}{R^2} f^{'}(R - c_{\mathrm{p}}t)] \tag{8}$$

$$\ddot{u} = \frac{\partial^2 u}{\partial t^2} = \frac{c_{\mathrm{p}}^2}{R} f^{'''}(R - c_{\mathrm{p}}t) - \frac{c_{\mathrm{p}}^2}{R^2} f^{''}(R - c_{\mathrm{p}}t) \tag{9}$$

$$\frac{\partial \sigma}{\partial t} = -c_{\mathrm{p}} \frac{\lambda + 2\mu}{R} f^{'''}(R - c_{\mathrm{p}}t) + c_{\mathrm{p}} \frac{4\mu}{R^2} f^{''}(R - c_{\mathrm{p}}t) - c_{\mathrm{p}} \frac{4\mu}{R^3} f^{'}(R - c_{\mathrm{p}}t) \tag{10}$$

Comparing with Eq.(3), the relationship between normal stress σ and displacement u can be obtained as follows.

$$\sigma + \frac{R}{c_{\mathrm{p}}}\dot{\sigma} = -\frac{4G}{R}[u + \frac{R}{c_{\mathrm{p}}}\dot{u} + \frac{\rho R^2}{4G}\ddot{u}] \tag{11}$$

Equation (11) is 3D artificial boundary function in the normal direction, where, $G=\mu$ is the shear modulus and ρ is the mass density of the medium. In deriving Eq. (11), the following expression was used.

$$\lambda + 2\mu = \rho c_{\mathrm{p}}^2 \tag{12}$$

As time tends to infinite, the 3D normal boundary Eq.(11) becomes

$$\sigma = -\frac{4G}{R}u \tag{13}$$

Equation (13) is the static boundary condition (Xu, 1990), which represents the relationship between displacement and stress near the cavity when the spherical cavity in an elastic infinite space is subjected to uniform pressure.

2.2 Numerical simulation technique on the normal boundary

The infinite homogenous medium is truncated by introducing artificial boundaries. At the truncating position on the boundaries, a continuous spring-dashpot-lumped mass system is set up, as shown in Fig.1.

The equation of motion of the physical system shown in Fig.1 is

$$Ku_{\mathrm{R}} + C(\dot{u}_{\mathrm{R}} - \dot{u}_{\mathrm{M}}) = \sigma \tag{14}$$

$$m\ddot{u}_{\mathrm{M}} + C(\dot{u}_{\mathrm{M}} - \dot{u}_{\mathrm{R}}) = 0 \tag{15}$$

The operators u_{R} and u_{M} in Eqs.(14) and (15) represent the displacements along the load direction on the boundary node and lumped mass, respectively. The following equations are obtained from Eq.(14).

$$\dot{u}_{\mathrm{M}} = \frac{1}{C}(Ku_{\mathrm{R}} + C\dot{u}_{\mathrm{R}} - \sigma) \tag{16}$$

$$\ddot{u}_{\mathrm{M}} = \frac{1}{C}(K\dot{u}_{\mathrm{R}} + C\ddot{u}_{\mathrm{R}} - \dot{\sigma}) \tag{17}$$

Substituting Eqs.(16) and (17) into Eq.(15), the differential function is obtained, which meets the requirement of the node's stress equilibrium and displacement continuity on the boundary of the physical system.

$$\sigma + \frac{M}{C}\frac{\partial \sigma}{\partial t} = K[u_{\mathrm{R}} + \frac{M}{C}\frac{\partial u_{\mathrm{R}}}{\partial t} + \frac{M}{K}\frac{\partial^2 u_{\mathrm{R}}}{\partial t^2}] \tag{18}$$

From Eqs.(11) and (18), expressions for the equivalent distributed stiffness, damping and mass can be found as follows:

$$K = \frac{4G}{R};\ C = \rho c_{\mathrm{p}};\ M = \rho R \tag{19}$$

thus, the conditions for stress and displacement on the boundary are identical with those of the original homogenous medium. The 3D VSAB can be achieved by simply using the corresponding spring, dashpot and lumped mass elements. The continuously distributed physics constants must be discretized according to rules in FEM analysis. For example, any parameter on the normal boundary can be taken as the product of the relevant value obtained from Eq.(19) and the grid area corresponding to the node.

In numerical implementation, the 3D artificial boundary can be set up by using the corresponding spring and dashpot only, ignoring the concentrated mass, such as shown in Fig.2. It has been shown from numerical examples that such simplification results in a minor effect on the numerical precision for most situations.

3 3D VSAB condition in tangential direction

3.1 Boundary equation in tangential direction

The dynamic displacement for spherical shear waves (S wave) can be approximately expressed in spherical coordinates by the following equation (Aki, 1980).

$$u(R,t) = \frac{1}{R} f(R - c_{\mathrm{s}}t) + \frac{1}{R} g(R + c_{\mathrm{s}}t) \tag{20}$$

in which c_{s} is the shear wave's velocity of the medium. The first and second items on the right side of Eq. (2) represent the scattering and converging waves, respectively.

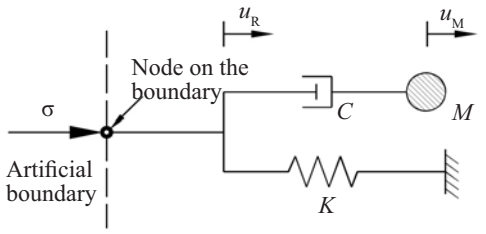

Fig. 1 Physical component applied on the normal boundary

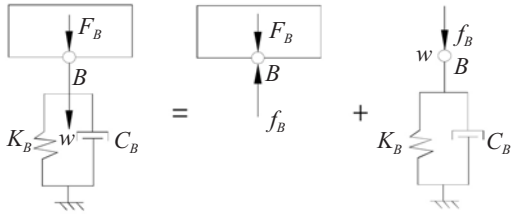

Fig. 2 Artificial boundaries and isolated bodies

Next, the spherically scattering shear wave is considered. The displacement in the tangential direction of the wave front can be expressed as:

$$u(R,t)=\frac{1}{R}f(R-c_s t) \tag{21}$$

The shear strain and shear stress can be derived from Eq.(21) as:

$$\gamma(R,t)=\frac{\partial u}{\partial R}-\frac{u}{R}=-\frac{2}{R^2}f(R-c_s t)+\frac{1}{R}f'(R-c_s t) \tag{22}$$

$$\tau(R,t)=G\gamma=G[-\frac{2}{R^2}f(R-c_s t)+\frac{1}{R}f'(R-c_s t)] \tag{23}$$

The velocity of a point of at a radial coordinate of R is

$$\dot{u}=\frac{\partial u(R,t)}{\partial t}=-\frac{c_s}{R}f'(R-c_s t) \tag{24}$$

From Eqs.(22), (23) and (24), the stress on the wave front is obtained.

$$\tau(R,t)=-\frac{2G}{R}u(R,t)-\rho c_s \dot{u}(R,t) \tag{25}$$

Equation (25) is the 3D artificial boundary condition in the tangential direction. It expresses the relationship between the stress and displacement on the wave front in the tangential direction. In deriving Eq.(25) $G=\rho c_s^2$ had been used.

3.2 Numerical simulation technique on the boundary in tangential direction

The 3D artificial boundary function in the tangential direction expressed by Eq.(25) implies a parallel-connected spring-dashpot system. The corresponding parameters of the physical components are

$$K=\frac{2G}{R};\ C=\rho c_s \tag{26}$$

As in the previous section, in the general FEM analysis program, any parameter on the boundary in the tangential direction can be taken as the product of the relevant value obtained from Eq.(26) and the grid area corresponding to the corresponding node.

4 Application of 3D VSAB

To simulate the condition of a practical continuous medium, Eq.(19) and Eq.(26) provide the parameters of the physical components applied in the normal and tangential directions of the artificial boundary. The mass M of the physical component on the normal boundary is joined with the dashpot. Obviously, it is an instable system, which is shown in Fig.1. It is not convenient for use in modeling and computing. To simplify the model, the mass component is neglected and the end of the dashpot is fixed. Thus, the artificial boundary with a viscous dashpot and spring is constructed, which is the Viscous-Spring Boundary. The effectiveness and accuracy of this boundary will be proven in the following examples. Note that the VSAB provides a simulation of the distributed stress condition on the artificial boundary. Therefore, it is a type of continuously distributed artificial boundary condition. The surface of the artificial boundary will be discretized when the computed domain on the boundary is discretized. The physical components of the continuous boundary can be changed into a coupled artificial boundary via the shape functions of FEM directly, and the consistent VSAB is achieved (Liu, 1997, 1998). It can also change into an uncoupled artificial boundary via the lumped parameters, resulting in a lumped VSAB, which can then be used. The detailed implementation method is shown in Fig.3. In Fig.3, the X and Y coordinates are both in the tangential directions and Z is in the normal direction. The parameters of the physical items on the nodes of the VSAB can be obtained from Eq. (27).

$$\left.\begin{aligned} K_1&=K_2=\frac{2G}{R}A\\ C_1&=C_2=\rho c_s A\\ K_3&=\frac{4G}{R}A\\ C_3&=\rho c_p A \end{aligned}\right\} \tag{27}$$

where A is the total area of all elements around the node considered on the boundary, for instance for the status

shown in Fig.3, we have $A=A_1+A_2+A_3+A_4$.

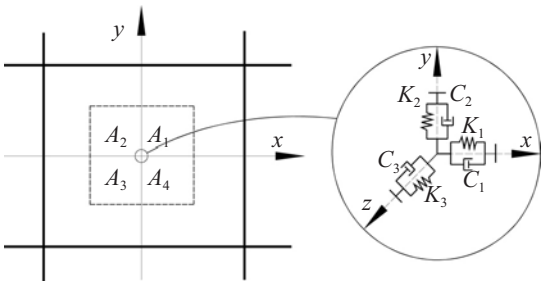

Fig. 3 Sketch of 3D VSAB

The above discussion refers to the full space and spherically symmetrical wave motion. However, in most practical situations, problems to be treated are in the half space and are nonsymmetrical. Moreover, low-frequency and the static state must be considered in many cases. The numerical parameters obtained from Eq.(27) are not available for general situations. Therefore, Eq.(27) is modified as Eq.(28):

$$\left.\begin{aligned} K_1 &= K_2 = \frac{\alpha_T G}{R} A \\ C_1 &= C_2 = \rho c_s A \\ K_3 &= \frac{\alpha_N G}{R} A \\ C_3 &= \rho c_p A \end{aligned}\right\} \tag{28}$$

where, α_T and α_N are modified coefficients in the tangential and normal directions, respectively. R is the distance between the load point and the boundary, which takes the approximate value of the perpendicular distance from the load point to the boundary.

It can be found that via the modified parameters given in Eq.(28), the half-space, low-frequency and static component in wave motion problem, especially SSI problem, can be satisfied.

The modified parameters in Eq. (28) can be determined from the parameter analysis and some example tests. The parameter analysis shows that the numerical solution only slightly varies with the change of the modified parameters around the recommended value given in Table 1. A viscous boundary is a result of a plane wave problem and VSAB is a 3D problem, in which the geometry spreading and scattering effects must be taken into account. Therefore, VSAB is more accurate than a viscous boundary.

Table 1 Recommended value of α_T and α_N

Modified parameters	Value range	Recommended value
α_N	1.0-2.0	1.33
α_T	0.5-1.0	0.67

5 Examples of numerical simulation

To verify the accuracy and reliability of the proposed 3D VSAB, four typical wave motion problems are examined as follows. The first example is an explosive source in an unbounded space, i.e, it is a spherically symmetric problem. The load is a dilated stress wave. The condition of this example is the same as the basis for the theory introduced in this paper. The second example is an inner-source problem. It is also a full infinite domain problem, but the load is concentrated in one direction. The third example is the Lamb problem, i.e., under a concentrated load on the half space surface. The last example is a half-infinite domain problem under several forces. In the first and the last examples, the generalized solution will be developed, while for the other examples, analytical solutions are available. In the second example, parameter analysis will be conducted and the value of the modified coefficients will be discussed. By presenting the solutions obtained under different artificial boundary conditions, the accuracy and applicability of 3D VSAB are identified.

5.1 Explosive-source problem

In this example, the wave motion caused by blasting in an homogeneous, isotropic and linear elastic infinite medium is studied. The model is an explosive-source model with spherically symmetrical coordinates. The explosive source is located at the origin point (0, 0, 0). There is a fluid cavity of 0.3m thickness between the dynamite and the medium. The velocity of shear wave of the medium is assumed to be C_s=500m/s, the mass density ρ=1800kg/m^3 and the Poisson's ratio ν=0.25. The time interval Δt=10μs is used. The dynamite part is meshed as Eulerian grids and the others are Lagrangian grids. Due to the spherical symmetry, only a one-eighth sphere, with R from 0 to 1m as shown in Fig.4, is needed for the finite element model. The parameters of α_T and α_N take the values of 2.0 and 4.0 without modification. The radius values of the observation points are 0.4m and 0.8m.

The displacement of the observed point is in the direction of the radius. The generalized solution is obtained by a model of R_{max}=10, which is much bigger than the model with VSAB. The corresponding numerical solutions are obtained by different boundaries, as shown in Fig.5. From the figures, it is seen that the 3D VSAB has good accuracy. The displacement response in the other direction is the same as shown in the figures.

The modified coefficients α_T and α_N were taken as the theoretical value. This implies that for this case, no modification of the parameters of Eq.(27) is needed. The explosive-source problem is a high-frequency problem and the shock wave is a dilated wave. The condition is the same as in the theoretical case. Therefore, it shows that the solutions of the derived equations are correct.

From the solution, it is also found that the viscous boundary has a good accuracy for high frequency problem. Nevertheless, it is not known whether the proposed 3D VSAB along with the recommendation of the modified coefficients of α_T and α_N can be confidently applied in the other situations.

5.2 Inner-source problem

In this example, the wave motion caused by a concentrated force in homogeneous, isotropic and linear elastic full infinite medium is studied. The Cartesian coordinates are adopted. The concentrated force is applied at the origin point (0, 0, 0) as shown in Fig.6. The range of the numerical computed object takes a cubic volume, with X, Y and Z all from –50m to 50m, and the grid size of $\Delta X=\Delta Y=\Delta Z=5$m. The coordinate of the observed points are $X=Y=Z=5$m and $X=20$m, $Y=Z=0$. The time interval $\Delta t=0.003$s is used for this example, and a large quarter model is not needed as in the explosive-source problem using symmetry, so a small full model is adopted.

The property of the medium is the same as in example 5.1. To explore the influence of the variety of the modified coefficients, different α_T values of 1/2, 2/3, 1.0, 4/3, 5/3 and 2.0 are used, while is twice the value of α_T, and R = 50m.

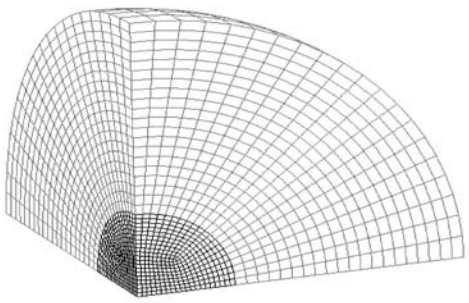

Fig. 4 Finite element model

Theoretically, it will be more accurate in numerical simulations if the spherical model is used for the artificial boundary, as shown in Fig.4. However, a plane and straight boundary is used for convenience in modeling. The direction of the boundary is perpendicular with the Cartesian coordinates. A rectangular computing domain is cut off in the space. Furthermore, the physical parameter of the distance R in the artificial boundary is taken as the shortest distance between the origin and the plane of the boundary uniformly, instead of the distance between the origin of the coordinates and the nodes on the boundary. Thus, each parameter on the plane and straight artificial boundary is identical. Therefore, R= 50m is assumed in this example.

The analytical solution under δ (Dirac) load function is obtained by integrating the basic solution of the inner-source problem (Pekeris, 1955).

The δ load function is expressed as

$$\delta(\tau)=1.6\times10^{10}[G_4(\tau)-4G_4(\tau-\frac{1}{4})+6G_4(\tau-\frac{1}{2}) -4G_4(\tau-\frac{3}{4})+G_4(\tau-1)] \tag{29}$$

$$G_4(\tau)=\tau^3H(\tau),\quad \tau=\frac{t}{T}$$

where T is the load time duration, and $H(\tau)$ is the Heaviside ladder function.

The displacement time histories of the observed points along the Z direction obtained from analytical method and numerical analysis with different artificial boundaries, including the proposed 3D VSAB, viscous boundary and fixed boundary, are shown in Fig.7. From the figure, it is seen that the displacement drift caused by the viscous boundary is obvious as in the Lamb problem, but the 3D VSAB gives the best accuracy among all the artificial boundaries considered.

Moreover, from Fig. 7, it is seen that in this case, where the problem of full infinite space is treated, and analyzed using a cubic model, the best accuracy of

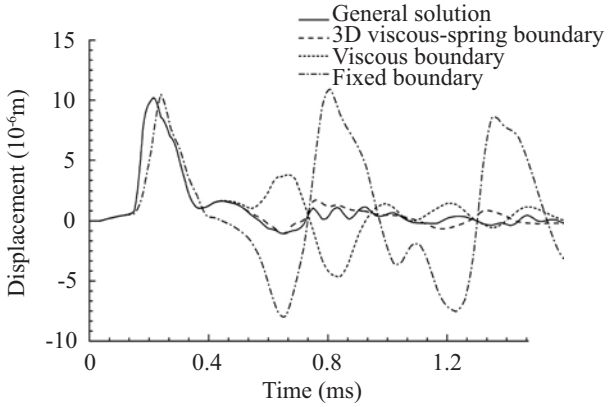

(a) For observation point, R=0.4

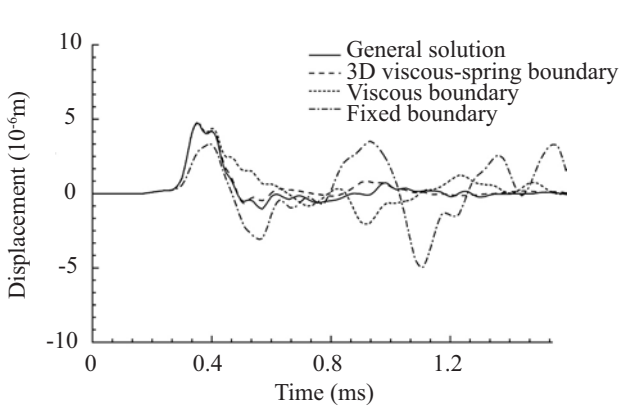

(b) For observation point, R=0.8

Fig. 5 Displacement time history of the explosive-source problem

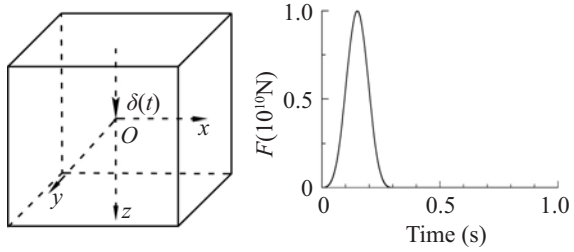

(a) Inner-source model (b) δ load

Fig. 6 Inner-source problem model and the δ load curve

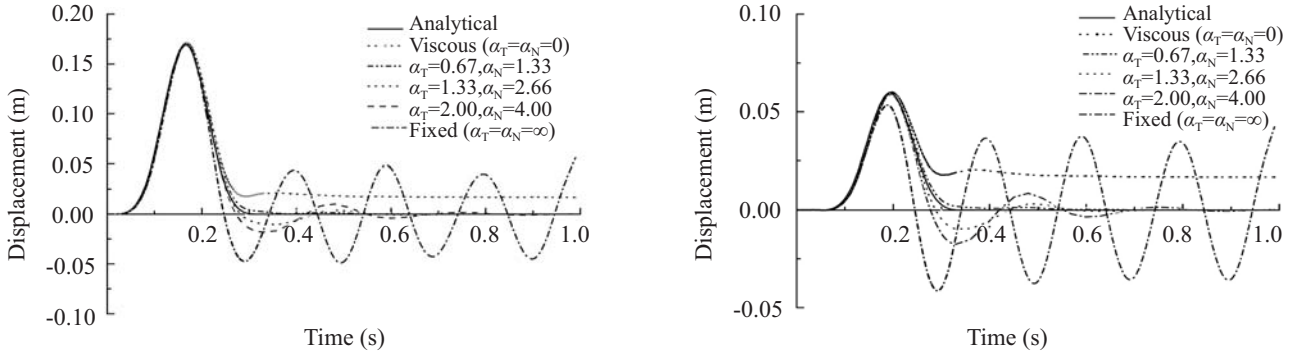

(a) For observation point *A* (5, 5, 5) (b) For observation point *B* (20,0,0)

Fig. 7 Displacement time histories of the inner-source problem

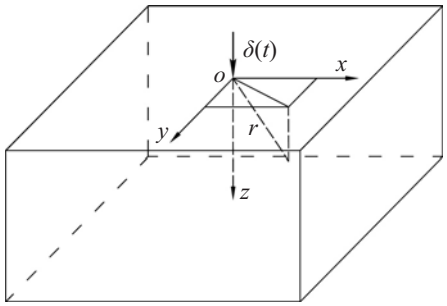

Fig. 8 Lamb problem model

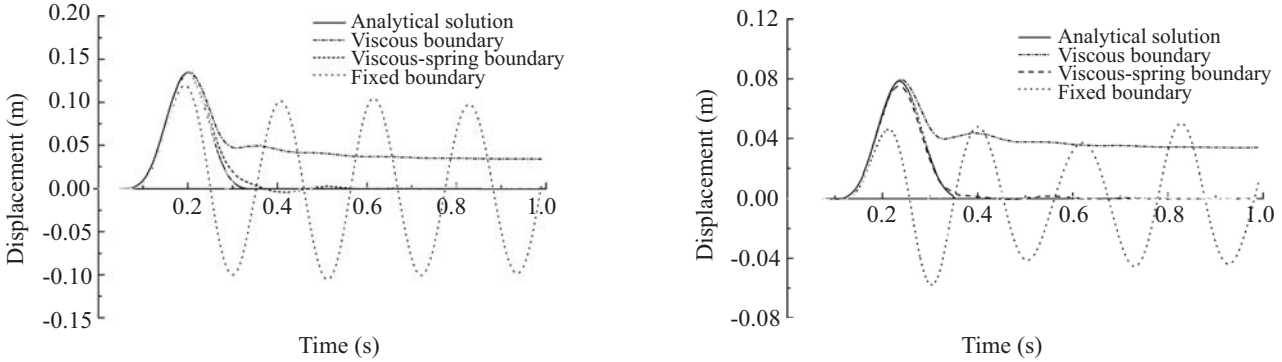

(a) For observation point *A* (20, 0, 0) (b) For observation point *B* (35, 0, 0)

Fig. 9 Displacement time histories of the Lamb problem

the numerical analyses is achieved when the modified coefficients are taken as the recommended values of α_T =2/3 and α_N =4/3 as given in Table 1. It can be proven that the values of the modified coefficients α_T and α_N are independent of the element grid size, the time interval and other computational factors involved in the finite element analysis procedure. The numerical error occurred for each artificial boundary shown in Fig.7 resulted from both the artificial boundary deficiency, and the finite element procedure. They are two independent aspects.

5.3 Lamb problem

This example is the surface source problem of Lamb, in a homogeneous and isotropic semi-infinite space with a vertical concentrated force of δ function on the free surface, as shown in Fig.8. The load δ is the same as in example 5.2.

In this example, the analytical solution can be obtained by integrating the basic solution of the Lamb problem (Pekeris, 1955; Wang, 2002).

The range of the numerically computed object is taken as: -50m≤X≤50m, -50m≤Y≤50m, and -50m≤Z≤0; the other parameters of the model are the same as in example 5.2. The observed item is the vertical displacement response of the nodes A(20, 0, 0) and B(35, 0, 0) on the free surface. The parameters of and α_N are also taken as the recommended values of 2/3 and 4/3, respectively.

The time histories of the displacement responses of observed points A and B are shown in Fig.9. As in example 5.2, the viscous boundary causes obvious displacement drift at the observed points, particularily for observation point B, which is closer to the artificial boundary than point A, while the proposed. 3D VSAB gives much better accuracy. The fixed boundary, the worst boundary, may cause enormous oscillation when the frequency of the load near to the natural frequency of the system is analyzed. The results reveal that the recommended modified parameters are also suitable for the concentrated load in half-infinite space.

5.4 Torsion and bending problem

This example is the surface source problem of a few forces in or perpendicular to the half-space surface plane inducing torsional and bending moment, which is shown in Fig.10. F is δ function and is the same as example 5.2.

The parameters of the model are the same as in example 5.3. The observed item is at a point A(25, 0, 0) on the free surface . The recommended values for the parameters of α_T and α_N are the same as those used in examples of 5.2 and 5.3. The forces, F, are at points B (5, 0, 0) and C (-5, 0, 0).

The displacement time histories at the observed point A are shown in Figs.11 and 12 for torsional and bending models, respectively. From the results, it is concluded that 3D VSAB has a wide applicable range. It also simulates the problem of rotary and bending moment on the surface of semi-infinite space very well.

The above examples only show the results in the main direction. The results from other directions have the same features as the main direction.

From these examples, it is shown that the viscous-spring boundary can be directly used in the dilated wave problem in the full infinite space. When the boundary is used in the concentrated load, rotary and bending load problem in half or full infinite space, the boundary is more accurate with the modified parameters α_T and α_N. The two modified parameters can take the value of 2/3 and 4/3, respectively. The parameter analysis in example

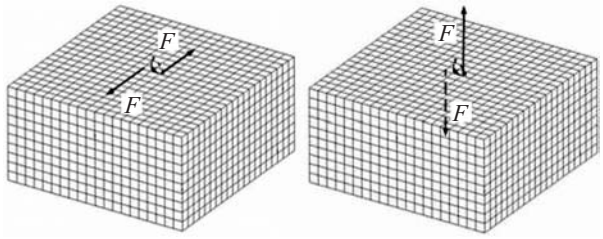

(a) Torsion (b) Bending

Fig. 10 Torsion and bending model

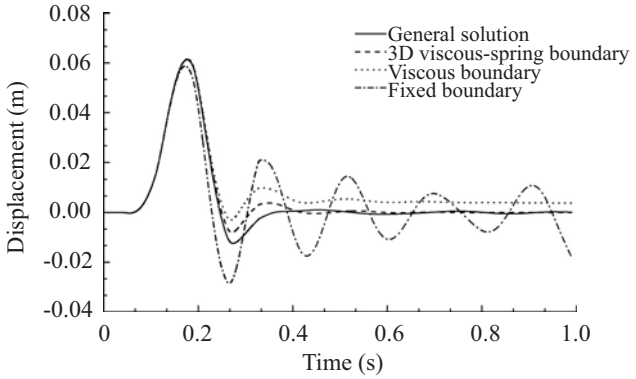

Fig. 11 Displacement time histories at point A (25, 0, 0) in direction of the couple of forces (Y) of rotary problem

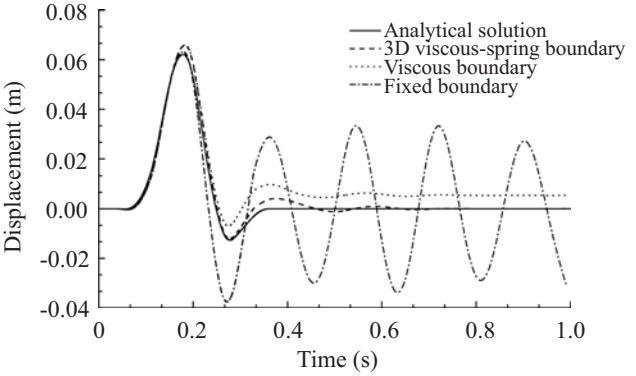

Fig. 12 Displacement time histories at point A (25, 0, 0) in direction of the couple of forces (Z) of bending problem

5.2 indicates that the accuracy of the viscous-spring boundary is better than the viscous boundary and fixed boundary even when the modified parameters take the unapt values. The 3D viscous spring boundary has a good stability.

6 Conclusions

To develop an effective, accurate and convenient 3D artificial boundary, simulating wave motion and the soil-structure interaction in the infinite and half-infinite medium is important. Based on the elastic wave theory, a 3D VSAB in the time domain is proposed in this paper. The proposed 3D VSAB consists of an unit of typical spring-dashpot in each direction, and the modified coefficients for the spring-dashpot parameters are also recommended. The modified parameters have been studied via parameter analysis. Four numerical examples are provided to illustrate the efficiency and accuracy of the proposed 3D VSAB. The examples consider different situations: full space and half space, high frequency and low frequency of the loading, spherically symmetrical domain and rectangular domain, etc. The following conclusions are drawn.

(1) The numerical examples demonstrate that by using the proposed 3D VSAB along with the recommended modified coefficients of α_T and α_N , high numerical precision and adequate stability can be achieved.

(2) The proposed 3D VSAB is better than the generally used viscous boundary, but not always better than all other local artificial boundaries, such as the multi-transmitting boundary suggested by Liao ZP *et al*.. However, the 3D VSAB is simple in physical concept and it can be conveniently incorporated in the general finite element program for the study of dynamic soil-structure interaction problems.

The proposed VSAB has been examined only for linear, homogeneous unbounded space problems, and internal excitation. Its application to layered soil, nonlinear performance and seismic response analysis etc. should be studied further. The application and subroutines for a general finite element program should be studied in the future.

References

Aki K and Richards PG (1980), *Quantitative Seismology Theory and Methods I*, Freeman and Company, WH.

Chen SL and Liao ZP (2003), "Multi-transmitting Formula for Attenuating Waves," *Acta seismologica sinica*, **16**(3): 283-291.

Deeks AJ and Randolph MF (1994), "Axisymmetric Time-domain Transmitting Boundaries," *Journal of Engineering Mechanics*, ASCE, **120**(1): 25-42.

Foreman MG (1986), "An Accuracy Analysis of Boundary Conditions for the Forced Shallow Water Equations," *Journal of Computational Physics*, **64**: 334-367.

Higdon RL (1986), "Absorbing Boundary Conditions for Difference Approximations to the Multi-dimensional Wave Equation," *Mathematics of Computation*, **47**: 437-459.

Jing LP and Liao ZP(2000), "Combination of Local and Global Artificial Boundary Condition," *Earthquake Engineering and Engineering Vibration*, **20**(3): 8-14. (in Chinese)

Kausel E (1988), "Local Transmitting Boundaries," *Journal of Engineering Mechanics,* ASCE, **114**(6): 1011-1027.

Keys RG (1985), "Absorbing Boundary Conditions for Acoustic Media," *Geophysics,* **50**: 892-902.

Liao ZP (1996), "Extrapolation Nonreflecting Boundary Conditions," *Wave Motion*, **24**: 117-138.

Liao ZP (1997), "Numerical Simulation of Near-field Wave Motion," *Advances in Mechanics,* **27**(2): 193-212.

Liao ZP (2002), *Introduction to Wave Motion Theories in Engineering*, China Academic Press, Beijing. (in Chinese)

Liu JB and Lu YD (1997), "A Direct Method for Analysis of Dynamic Soil-structure Interaction Based on Interface Idea," Zhang CH and Wolf JP ed, *Dynamic Soil-Structure Interaction*, International Academic Publishers, 258-273.

Liu JB and Lu YD (1998), "A Direct Method for Analysis of Dynamic Soil-structure Interaction,," *China Civil Engineering Journal*, **31**(3): 55-64. (in Chinese)

Liu JB, Wang ZY and Zhang KF (2002), "3D Finite Element Analysis of Large Dynamic Machine Foundation Considering Soil-structure Interaction," *Engineering Mechanics*, **19**(3): 34-38. (in Chinese)

Lysmer J and Kulemeyer RL (1969), "Finite Dynamic Model for Infinite Media," *Journal of Engineering Mechanics,* ASCE, **95**: 759-877.

Pekeris CL (1955), *Proceedings of the national academy of sciences* USA, **41**: 469.

Smith WD (1974), "A Nonreflecting Plane Boundary for Wave Propagation Problems," *Journal of Computational Physics,* **15**(4): 492-503.

The National Standard GB50267-97 (1998), "Code for Seismic Design of Nuclear Power Plants," China Building Industry Press, Beijing. (in Chinese)

Underwood P and Green TL (1981), "Doubly Asymptotic Boundary-element Analysis of Dynamic Soil-structure Interaction," *International Journal of Solids and Structures,* **17**: 687-697.

Wang ZY (2002), "Computational Theory of Dynamic Response of Large Structure-soil Systems and Its Application," *Dissertation for PhD*. Tsinghua University, Beijing. (in Chinese)

Wolf JP (1986), "A Comparison of Time-domain

Transmitting Boundaries," *Earthquake Engineering and Structural Dynamics,* **14**: 655-673.

Wolf JP (1988), *Soil-structure-interaction Analysis in Time Domain*, Prentice-Hall, Englewood Cliffs, NJ.

Wolf JP and Paronesso A (1992), "Lumped-parameter Model for Rigid Cylindrical Foundation Embedded in Soil Layer on Rigid Rock," *Earthquake Engineering and Structural Dynamics*, **21**: 1132-1144.

Wolf JP and Song CM (1995), "Doubly Asymptotic Multi-directional Transmitting Boundary for Dynamic Unbounded Media-structure Interaction Analysis," *Earthquake Engineering and Structural Dynamics*, **24**: 175-188.

Xu ZL (1990), *Elasticity Mechanics*, Higher Education Press, Beijing. (in Chinese)

Yan JY, Jin F, Xu YJ *et al*. (2003), "A Seismic Free Field Input Model for FE-SBFE Coupling in Time Domain", *Earthquake Engineeing and Engineering Vibration*, **2**(1):51-58

Zhao CB, Zhang CH and Zhang GD (1989), "Analysis of 3D Foundation Wave Problems by Mapped Dynamic Infinite Elements," *Science in China Series A,* **32**(4): 479-491.